

LUMINESCENT DYE MOLECULES FOR NEW PHOTONIC ANTENNAE

*¹Abdullahi K., ²Sulaiman M.

¹Department of Integrated Science, Isa Kaita College of Education Dutsin-ma, Katsina State,

²Department of Chemistry, Government Pilot Secondary School Daura, Katsina State, Nigeria,

*Corresponding authors' email: danabdukabir@gmail.com

ABSTRACT

A zinc dipyrin complex with a structural and functional design, that mimics the natural photonic antenna of a green plant, has been synthesized and incorporated into new designed model of mesoporous silica. The dye complex is composed of two dipyrromethene ligands which are connected to a central zinc(II) metal ion through the four nitrogen atoms. The dye complex has been characterized using various spectroscopic techniques, ¹HNMR, IR, and X-ray crystallography to elucidate their structure. UV-vis absorption and fluorescence spectroscopy were used to determine the optical properties of the dye before its encapsulation into the silica framework, and after being trapped in the silica pores. A comparison of the results obtained shows that the silica pores have a significant effect on the fluorescence quantum yield, the excited state lifetime, and the emission of the encapsulated dye molecules.

Keywords: Zinc, dipyrromethane, complex, mesoporous silica, photonic antennae, host-guest, light harvesting, Porphyrin

INTRODUCTION

In natural photosynthesis, light from the sun is absorbed by the pigmenting material located in the chloroplast of a green plant and conveyed to the reaction Centre, usually within the membrane where catalysis takes place, in which carbon dioxide and water are used to produce chemical feedstocks in the form of sugars. However, in the process, oxygen is produced which is an essential condition for all animal and human life, as without oxygen only primitive organisms could have ever existed. Green leaves comprise numerous of such

well-organized 'antenna' devices which are composed of porphyrin dyes with alternating networks of single and double bonds, therefore the orbitals can delocalize the conjugated electrons and stabilize the structure. This property gives chlorophyll the ability to absorb sunlight. (Yu et al., 2019)

The basic structure of this natural antenna molecule comprises a central magnesium (II) ion surrounded by a porphyrin ring (four modified pyrrole subunits interconnected at the alpha carbon via methine bridges) and a hydrophobic tail (see Figure 1).

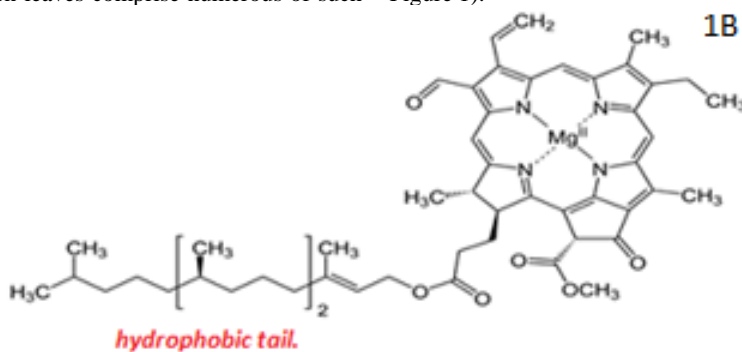


Figure 1: Showing the molecular structure of natural chlorophyll.

Much progress has been achieved in terms of understanding the functions, energetics, dynamics, compositions and structures of natural photosynthetic light harvesting arrays, even though some essential issues are yet resolved (Farràs & Cucinotta, 2017). The major chemistry behind has been identified at a sufficient level of understanding to allow the invention of artificial analogues that could promote technological advancement in solar energy conversions, molecular-based photoelectronics, generation of renewable fuel and electricity and a variety of other applications (Fang et al., 2018).

Many interesting researches mimic the antenna system of green plants by using nanostructured materials assembled via non-covalent interactions as in the chlorophyll-protein complexes present in green plants, intending to minimize non-radiative energy losses and maximize the efficiency of light absorption over the visible spectrum by dyes. Porphyrin has

been widely employed in synthetic light-harvesting systems, both alone and in combination with other accessory pigments to improve the spectral coverage. (Sazanovich et al., 2004). Generally, dipyrromethenes and their derivatives show weak fluorescence with quantum yield (Φ_F) below 1-2%. (Antina et al., 2017) However, due to the well-organized structural arrangement of porphyrins, dipyrromethene molecules can be effectively coordinated by ions of certain elements, forming intermolecular complexes with rigid structure and improved stability, which in turn result in fluorescence enhancement. (Dudina et al., 2014) For example, photonic of boron difluoride chelated dipyrromethene (BODIPY) has attracted great attention since 1968 when first synthesized by Treibs and Kreuzer (Bodio & Goze, 2019), because of its wide variety of applications in scientific fields which include biomedical applications, laser dyes, electroluminescent devices, photovoltaic cells etc. Dipyrromethene forms stable

chelates not only with boron(III) but also with ions of some d-block elements such as zinc(II) and copper(II), (Matsuoka & Nabeshima, 2018) these coordination complexes show strong absorption in the visible and near UV ranges. Even though only few literature studies have been reported about the spectral and luminescent properties of zinc(II) dipyrromethenes, the studies showed that zinc(II) and other d-block transition metals coordinated to dipyrromethene have some advantages over BODIPYs, such as sensitivity toward spectroscopic solvents and an easier self-assembling under mild conditions, (Vecchi et al., 2015) properties that favor their analytical application. This is because transition metal

centers are capable of coordinating two chromophoric dipyrromethene ligands with coordination numbers ranging from four to six. For example, M.W. Hosseini and coworkers recently reported the synthesis and photophysical analysis of zinc(II) and cadmium(II) chelates to α - β substituted dipyrins $[\text{Zn}(\text{dpm})_2]$, $[\text{Cd}(\text{dpm})_2]$; both of the complexes were found to have formed 1-, 2-, and 3D coordination polymers by self-assembly. The structural investigation revealed that cadmium(II) Centre can form penta- or hexa- coordination complexes in the presence of additional coordinating groups, (Béziau et al., 2013) therefore more prone to easier self-assembly into coordination polymers (see Figure 2).

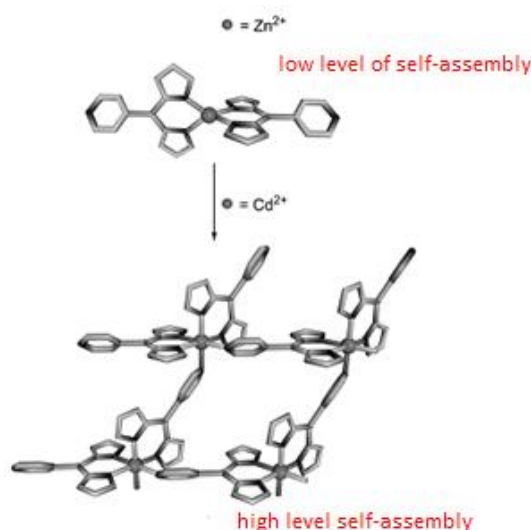


Figure 2: Schematic representation for the level of self-assembly in $[\text{Zn}(\text{dpm})_2]$ and $[\text{Cd}(\text{dpm})_2]$, complexes due to differences in their coordination numbers. Adapted from: *hem. Eur. J* (p 3216) by M.W Hossein (2013).

Consequently, research into the photonic and luminescence of these complexes is of great importance. The aim of this study was to design an artificial photonic antenna of Zinc (II) dipyrromethene complex (Figure 2) capable of absorbing light, transferring the resulting excitation to an energy sink and using the captured energy to initiate photo-induced energy and/or electron transfer. (Shoji & Tamiaki, 2019) Even though zinc(II) is optically inert (d^{10} electron configuration), many zinc porphyrins have been utilized to create light-harvesting systems and the structural role of this metal ion proved to play an important part in conferring further stability to both porphyrin- and dipyrromethene-based structures and allows the construction of poly-coordinated assemblies. (Davila, Harriman, & Milgrom, 1987).

Host-guest chemistry provides an effective way of achieving such organized assemblies, which involves inserting a luminescent guest species into normally non-emissive sol-gel host material, resulting in optical systems that preserve both the guest's photophysical properties and the host's mechanical and structural characteristics (Binnemans, 2009). Such materials are characterized by large surface areas and

well-defined pore radius distribution which enable them to encompass smaller guest materials, such as donor/acceptor chromophores. The interaction among them leads to the formation of new supramolecular species, usually with improved optical properties concerning the separate individual components (Badamasi et al.). Examples of such structures are zeolites and a newly developed class of mesoporous silica, such as MCM-41 (with a hexagonal porous arrangement) and MCM-48 (with a cubic arrangement of the mesopores) (Leśniewski, 2016). A wide variety of small organic dyes as well as metal-organic complexes can be incorporated into these microporous and mesoporous structures as guests. Mostly the synthesis of mesoporous silica is based on sol-gel hydrolysis of silica precursor, mainly tetraethyl orthosilicate (TEOS) around a surfactant-based template, typically made of polyethylene/polypropylene glycol copolymers, the most commonly used being Pluronic P123. The hydrolysis of silica precursor is followed by the condensation process by the formation of Si-O-Si bonds to produce a spherical nanoparticle of mesoporous silica (see Figure 3).

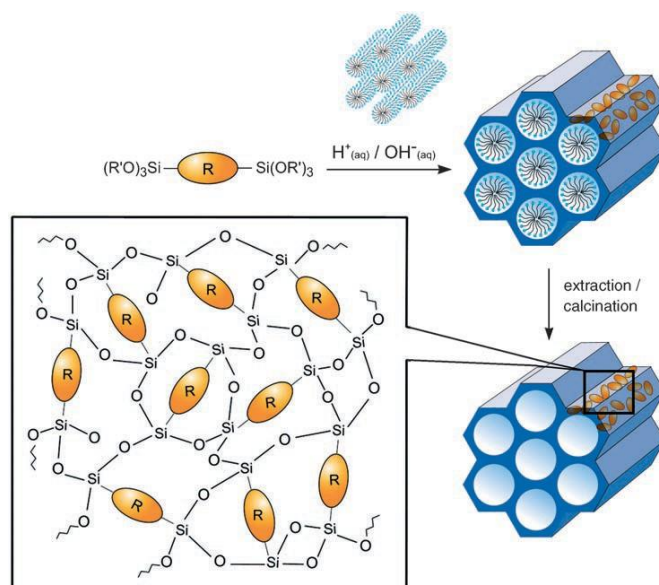


Figure 3: schematic representation of the general synthetic pathway of the mesoporous silica. R= (organic bridge of the dye). Adapted from (M. Froba et al., 2006.)

Generally, the optical properties of dye molecules in solution are affected by solvent polarity, i.e. different solvents can cause change in the absorption and emission energies, depending on the stabilization effects that solvents cause on the excited states. Furthermore, an increase in the concentration of dyes in solution can bring about aggregation (i.e. an interaction of dye molecules with one another): this type of interaction also reduces the intensity of the dye absorption and emission. By using silica as a solid state dispersion medium, the optical properties of the dye can be preserved: this can be achieved by incorporation of the dye into the mesoporous silica, which plays the role of scaffold by dispersing the dye molecules in a homogenous distribution,

reducing intermolecular aggregation phenomena. Being the chromophore in the silica structure, the absorption and emission wavelengths of the dye over the visible spectrum can be tuned either to higher values (redshift), by increasing the concentration of the dye into the host and forcing aggregation to take place to a controlled extent or to lower values (blue shift), by decreasing the concentration of the dye (Jarman & Cucinotta, 2015). This can be achieved while the chemical structure, the homogeneity and the porosity of the mesoporous material along with the synthetic conditions such as the ionic strength, the pH and the temperature, are kept intact.

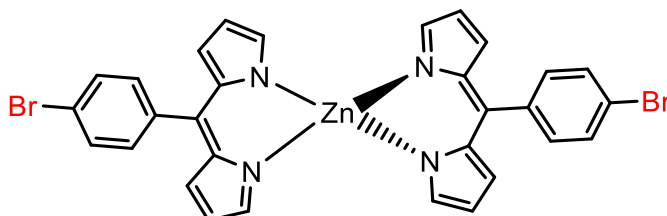


Figure 4: Structure of Zinc (II) dipyrromethene complex

Several attempts have been made and are still in progress to synthesize metal complexes and incorporate them into microporous and mesoporous materials, such as zeolites and mesoporous silica, using host-guest chemistry. Synthesis and confinement of photoactive species in zeolite pores have been reported in a quite high number of studies. In a recent article by GionCalzaferri and co-workers, it was found that the organic dye hostasol red (HR) could be incorporated into zeolite L (ZL) at ambient conditions and revealed strong absorption and luminescence in the 200-700 nm region, even though some variations have been observed in the optical property of the dye by changing the cationic nature of the zeolite (Devaux et al., 2014; Król, 2019). The results showed overall a positive response, in that the dye-zeolite hybrids obtained exhibit higher absorption and emission properties than the free dye, in the UV-visible spectrum. Another advantage of the host-guest approach is the possibility of manipulating the optical properties of the dye. However, the

main limitation of this approach is that zeolites have a very small pore size, usually less than 2 nm in diameter, which limits its use when large guest species need to be introduced. Another drawback to this method is represented by the impossibility of dye incorporation as part of the host structure itself: the harsh conditions required for the formation of zeolites, i.e. low pH, high temperature and pressure, would lead to degradation of the complex dye during the synthesis. (Insuwan, Jungstittwong, & Rangsiwatananon, 2015)

Because of such limitations in the use of zeolites as a host, researchers began to look at mesoporous silica materials, due to their larger pore sizes (approximately between 2-10 nm) and milder synthesis conditions. The first discovery of mesoporous silica was MCM-41 in 1992, by the Mobil Oil Company which reported the formation of mesoporous silica from a sol-gel synthetic method that makes use of pre-

assembled template to produce a porous structure. (Kumar, Malik, & Purohit, 2017)

S. Balasubramanian and G.R. Reddy successfully synthesized complexes of Ni(II) and Cu(II) with Schiff base ligands and incorporated them into MCM-41 mesoporous silica by post-grafting method. The results obtained show that both complexes responded positively in the UV-visible region: The Ni(II) complex showed an absorption band at 339 nm, whereas the Cu(II) complex showed a band with a maximum peak at 316 nm. (Ramanjaneya Reddy & Balasubramanian, 2015) Such values obtained confirmed that the complexes can retain their optical properties once in the silica, with strong absorption and emission of light in the UV-visible range, and can therefore be utilized for several important applications as in photocatalysis and light-emitting devices.

Synthesis and successful incorporation of a Zinc-HQ complex into mesoporous silica has also been reported, (Li et al., 2012) with outstanding optical stability and highly fluorescent emission of about 500 nm in the pH range of 3-10. This obtained fluorescent value can be used for drug delivery, cell imaging and many important biomedical applications. It was found that the photo luminescent property of Zinc(II) 8-hydroxyquinolate containing in the mesoporous silica nanoparticle depends on the concentration of Zinc-HQ in the mesoporous silica.

A limitation to using mesoporous silica is that its pores can only accommodate a small number of organic and organometallic dye molecules and also the host structure is completely comprised of silica, which limits its applications when interactions between the host and dyes species need to be sought and tailored.

The approach in this study employed a synthetic method developed by our research group which tackles these limitations, by synthesizing a hybridized dye-silica material, based on plain COK-12 silica as a model, with wide mesopores (6-7 nm) that can additionally accommodate large guest molecules and thus expanding the photochemical properties.

MATERIAL AND METHODS

All air and water-sensitive experiments were carried out under a nitrogen atmosphere using standard vacuum-line techniques. All chemicals were purchased commercially and used without further purification. "H₂O" refers to a high quality of water. DCM and acetonitrile used for photophysical measurements were spectroscopic grades and were used without further purification. Tin layer Chromatographic purification were performed on silica plates and visualized by UV lamp. ¹H NMR spectra were recorded on either Bruker 300MHz or 400MHz spectrometer operating at room temperature. Samples were prepared in 5 mm NMR tube using appropriate deuterated solvents. Chemical shifts are recorded relative to TMS and reported in ppm, coupling constants are in Hz and splitting pattern were abbreviated as (s) singlet, (d) doublet, (t) triplet and (m) multiplet.

Synthesis of Aryl Dipyrromethane

4-Bromo benzaldehyde (400mg, 2.16 mmol) was added to a degassed HCl (12M (1.2 mL, 0.36mmol)) and 7.82 mL of H₂O. It was then purged with nitrogen for 10 minutes to get rid of any unwanted gas such as oxygen. To this, pyrrole (10.7 mmol, 72 µL) was added under nitrogen, this cause the reaction mixture to turn white and cloudy. The reaction mixture was then allowed to stir for 5 hours at room temperature. The product was washed with 40 ml DCM and water, then the crude was filtered, separated and dried over Na₂SO₄, which led to the formation of grey-brown solid

product with a yield of 87% (634 mg, 2.1 mmol). The ¹H NMR data were in agreement with those reported in literature, for example by Dehean et al. (Rohand et al., 2007). ¹H NMR (300MHz, DMSO) δ= 7.84 (d, J_{HH}=7.3Hz, CH, Ar-Br), 7.23 (d, J_{HH}= 7.32, CH, Ar), 5.32 (s, 1H, methine), 6.08 (t, J_{HHH}=7.5 CH, pyrrole), 6.64 (d, J_{HH}=7.5 1H, pyrrole), 11.54 s, NH, pyrrole), 6.08 (t, J_{HHH}=7.5 CH, pyrrole), 6.64 (d, J_{HH}=7.5 1H, pyrrole), 11.54 (s, NH, pyrrole).

Oxidation and Complexation

To the dipyrromethane obtained above, (2.10 mmol, 624 mg) p-chloranil (550mg, 2.20 mmol) was added followed by dry DCM (42 mL); the solution was allowed to stir at room temperature for 24 hours under nitrogen after which the mixture turned dark brown. To the continued stirring reaction, (assuming 100%) diisopropyltriethylamine (5.25 mmol, 914 µL) was added, zinc acetate anhydrate (230 mg, 1.05 mmol) was first dissolved in 10 mL ethanol and the resulting solution was gently added into the reaction mixture and allowed to stir for 24 hour at room temperature and under nitrogen. No observable color change was obtained. The crude was then washed with brine (50 mL) and H₂O (2×50 mL), dried over MgSO₄ and rotary evaporated. Recrystallization was then followed, using DCM and 10 mL of petrol ether and then left in the fridge overnight. The dark brown solid sample (63% yield) was then taken for NMR, X-ray and UV-spectroscopic analysis. ¹H NMR (300MHz, CDCl₃) δ= 7.46 (d, J_{HH}=7.3Hz, CH, Ar-Br) 7.54 (d, J_{HH}=7.3Hz, CH-Ar), 7.46 (d, J_{HH}, =7.5Hz, 1H-pyrrole), 6.42 (t, J_{HHH}=7.5 Hz, CH-pyrrole), 6.71 (d, J_{HH}, =7.5 CH-pyrrole) 4.38 (s, 1H, methine), 7.46 (d, J_{HH}=7.3Hz, CH, Ar-Br) 7.54 (d, J_{HH}=7.3Hz, CH-Ar), 7.46 (d, J_{HH}, =7.5Hz, 1H-pyrrole), 6.42 (t, J_{HHH}=7.5 Hz, CH-pyrrole), 6.71 (d, J_{HH}, =7.5 CH-pyrrole) 4.38 (s, 1H, methane).

Conversion of Bromine Functional Group to Trialkoxysilane Br-Zinc dipyrromethane complex (0.15 mmol, 100 mg) was purged under nitrogen and dissolved in 10 mL dry THF and stirred to dissolve completely, the flask was then put in dry ice + acetone: this lowers the temperature to -78 °C, n-butyl lithium (0.6 mmol, 65 µL) was added drop wise and allowed to stir for 3 hours under same condition. A second flask was prepared after 3 hours, containing Tetraethyl orthosilicate, TEOS (1.05 mmol, 234 µL) dissolved in 10 mL dry THF at -78 °C and under nitrogen. The content of the first flask was then transferred completely into the second flask and allowed to stir for another 2 hours. The reaction was then quenched with 2 mL of water and allowed to warm to room temperature. The dark brown crude was then filtered, evaporated and separated by adding 20 mL DCM and 30 ML of water.

Doping The Silica Framework with Zn(dpm)₂ Dye

Pluronic, p-123 (190 mg, 0.032 mmol), citric acid monohydrate (182 mg, 0.86 mmol) and trisodium citrate dihydrate (172 mg, 0.6 mmol) were stirred in water at room temperature, for 1.5 h during which the solution turned clear. Silylated Zn(dpm)₂ dye (22 mg, 0.026 mmol) was first dissolved in (1300 µL) methanol in a separate vial and then added dropwise into the stirring mixture and allowed to stirred for 1 hour during which the solution turned brown. Sodium silicate solution (0.82 mmol, 1560 µL) was added drop wise to the reaction mixture and stirred for 15 minutes turning the reaction mixture a cloudy grey. This was then left uninterrupted for 24 hours during which a precipitate formed. The mixture was then filtered under vacuum and washed with water resulting in formation of a foam, which stopped on repeated washing. The filtrate was then dried in an oven and

overnight, a grey solid was formed which fluoresced under ultraviolet light.

RESULTS AND DISCUSSION

Synthesis of Dye and Material

Following the previously published procedures on the synthesis of zinc dipyrromethenes,⁴ as shown in scheme 1, the first stage was the synthesis of dipyrromethane ligand by acid-catalyzed (HCl) condensation of 4-bromobenzaldehyde with five equivalents of free pyrrole. Free pyrrole was used due to its strongly reduced hindrance compared to the substituted ones, while the bromine-substituted aldehyde was used because it can easily be converted to an alkoxy silane group, which is able to react with and be part of the silica network. The conversion of dipyrromethane to the corresponding dipyrromethene (which is the right form that can complex the metal) was achieved by oxidation of the later with tetrachloro-1,4-benzoquinone (p-chloranil) at room temperature under nitrogen. The Complexation was accomplished by reacting two equivalent dipyrromethenes with zinc acetate anhydrous salt, because the acetate group can easily swap with the dipyrromethene ligand, and diisopropyltriethylamine was used as a base to promote the deprotonation of the dipyrromethene. The bromine functional group was then converted to trialkoxysilane using a two steps reaction: first, was the treatment of the brominated Zn(dpm)₂ dye with *n*-butyl lithium at -78 °C, to form an aryl lithium intermediate and then treating the aryl lithium with a silicon-based electrophile, TEOS, in order to make the complex reactive toward silica (see experimental section). Each intermediate as well as the final product were characterized by NMR and IR spectroscopies. Additionally, the final crystal of the Zn(dpm)₂ complex formed was also analyzed by X-ray crystallography.

Incorporation of Zn(dpm)₂ Dye into Silica Framework

The network structure of a mesoporous silica comprises a large number of -Si-O-Si- bonds as shown in Figure 4. The incorporation of the dye into the silica matrix can take place simultaneously with formation of the mesoporous silica. The procedures for making of the silica porous materials are based on the condensation and hydrolysis of TEOS.

In this research work, we choose COK-12 model of mesoporous silica with large pore-size that can accommodate large number of guest dyes. A COK-12 mesoporous silica material was prepared according to the procedure developed by Cuccinota's research group, where by the silylated Zn(dpm)₂ was used as a dopant into pluronic 123, in water at neutral pH, citrate buffer made from citric acid monohydrate and trisodium citrate was used in order to lower the pH of sodium silicate and maintain the reaction environment at pH closer to 6.5 to avoid degradation during the reaction. Formation of mesoporous silica was accomplished upon addition of sodium silicate solution into the micellar system

Spectral Luminescence properties of Zn(dpm)₂ complex

The Zinc dipyrromethene complex was analyzed spectroscopically through UV-vis absorption and photoluminescence measurements (emission, lifetime and excitation) both in solution and in silica framework. The UV-vis absorption of the free dye was recorded in 10⁻⁶M acetonitrile, with maximum absorption of $\lambda_{max} = 480$ nm, as shown in figure 5A. The extent of aggregation in the dye molecules, at this concentration was also determined via Beer-Lambert plot of four different concentrations of the dye in acetonitrile solution, (i.e. 8×10⁻⁶M, 6×10⁻⁶M, 4×10⁻⁶M and 2×10⁻⁶M) which gave a straight line plot (Fig 5B). This proved that dyes do not aggregate at such low concentrations, as reported by numerous studies (Tolbin et al., 2017)

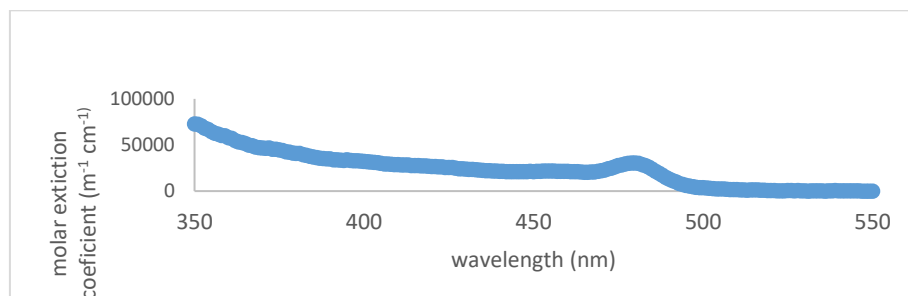


Figure 5a

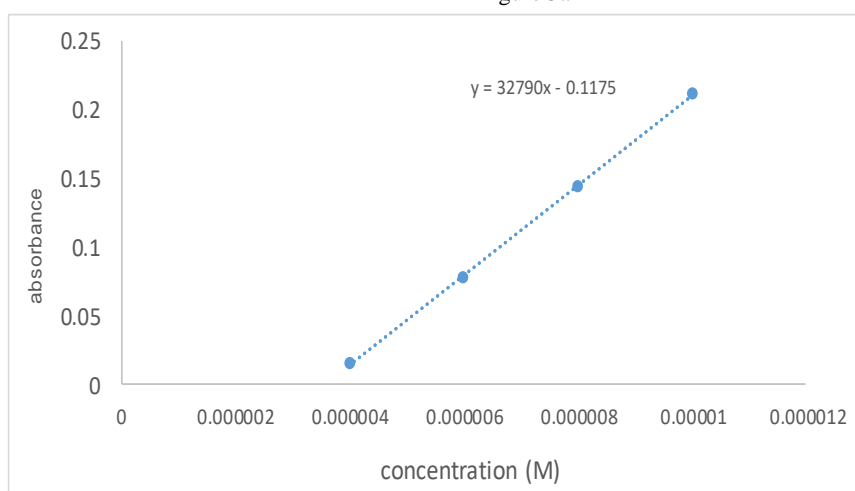


Figure 5b

Figure 5A and B, UV-vis absorption spectrum of Zn(dpm)2 dye recorded in a 10^{-6} M acetonitrile solution and Beer-Lambert plot of the dye in solution from four different concentrations, shown respectively. The fluorescence spectroscopy (excitation, excited state lifetime and emission) of the free dye in solution of cyclohexane are also reported and compared with luminescence properties of the dye in silica hybrid. The emission spectral plot of Zn(dpm)2 dye in cyclohexane solution and silica framework are reported in Figure 6a, showing maximum emission at about 505 nm in both spectra and the photoluminescence quantum yield (Φ_{PL}) of Zn(dpm)2 in silica was calculated to be 0.054 (5.4 %) which is about 8 times higher than the quantum yield of the free dye in cyclohexane, 0.007(0.7%). The excited state

lifetime of the dye in acetonitrile solution and silica, (see Figure 6b.) was found to be 2.3×10^{-9} s and 2.6×10^{-9} s respectively. The fluorescence rate (k_F) and non-radiative rate (k_{NR}) can also be determined using the relation: $\phi_f = k_F \tau$, and $(\tau = \frac{1}{k_F + k_{NR}})$,

Where ϕ_f = fluorescence quantum yield, τ = excited state lifetime,

k_F = fluorescence rate and k_{NR} = non-radiative rate.

By using the above relations, the k_{NR} , and k_F values of the dye in solution and in the silica framework can be determined. Table 1 shows the values of these parameters for dye both in solution and in silica.

Table1: Vales of parameters for dye both in solution and in silica

	k_F (s^{-1})	k_{NR} (s^{-1})	ϕ_f	τ (ns)
Dye in sol.	3.0×10^{-6}	4.3×10^{-8}	0.007	2.3
Dye in silica	2.0×10^{-7}	3.6×10^{-8}	0.054	2.6

Table 1. Showing the fluorescence rate (k_F), non-radiative rate (k_{NR}), quantum yield (ϕ_f) and excited state lifetime (τ) of Zn(dpm)2 both in solution and in the silica nanomatrix.

The above values obtained, for the dye both in solution and in silica, showed that the porous silica material has significantly affected the optical properties and the structure of the encapsulated dye. In order to assess the effect of mesoporous silica on photophysical and luminescence properties of the incorporated dye molecules, it is first important to understand how the physical status of dye molecules is being influenced when enclosed into the silica material. Aggregation, limited diffusion and restricted motion are generally the factors that

affect the properties of dye molecules encapsulated in silica material. Therefore, the fluorescence quantum yield (Φ_F) of Zn(dpm)2 in the silica matrix, is higher than the free dye in solution, because of the following roles played by the silica matrix:

First, the immobilization effect by the silica pores, restricts the free motion of the encapsulated dyes. This may be because the -O-Si-O- chain present in the silica can act as a barrier between the dye molecules to reduce their motion, hence limiting the possibility of aggregation, which is inversely related to the photoluminescence quantum yield.

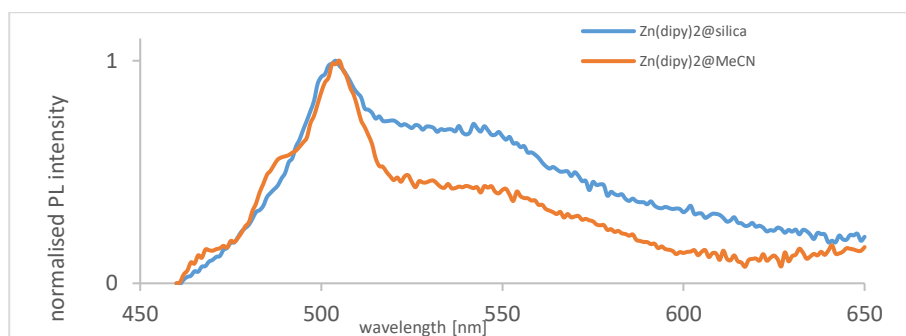


Figure 6a

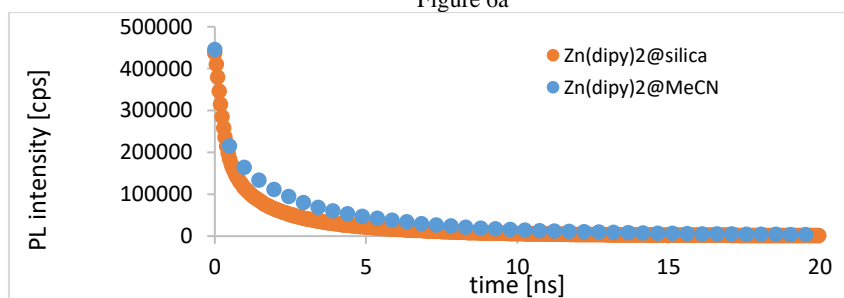


Figure 6b.

Figure 6(a) normalized emission spectra of Zn(dipy)2 dye in silica (blue) and in acetonitrile solution. (b) normalised excited state life-time of COK-12 silica hybrid, compared to the free dye in acetonitrile solution.

Second is the shielding effect by the silica porous material, which prevents the dye from being quenched by the surrounding materials and the solvent. It is reported that free dye in an aqueous solution suffers from dynamic quenching (a process that decreases fluorescence intensity of dyes) when it comes into contact with quenchers, e.g. molecular oxygen.²²

In the mesoporous silica, the extensive -O-Si-O- linkages play an important role in restricting the diffusion of atmospheric oxygen and therefore reduce the collision of oxygen with the encapsulated dye molecule. Therefore, less diffusion of quenchers into the system can induce an

enhancement of the fluorescence quantum yield of the dyes contained in the silica matrix.²³

The excitation spectrum of the dye in silica also indicated a significant red shift of about 50 nm as compared to the free

dye in acetonitrile solution (see Figure 7). This effect is also attributed to the aforementioned roles played by the silica scaffold

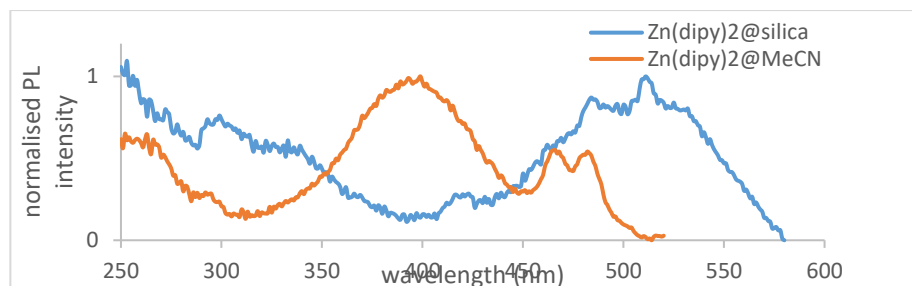


Figure 7: Normalized excitation spectra of Zn(dpm)2 encapsulated into silica compared to the free dye in acetonitrile solution. Conclusion

A complex of Zinc(II) with two identical dipyrromethene ligands has been synthesized, by acid-catalyzed condensation of pyrrole and aldehyde, oxidation and subsequent Complexation. The successful incorporation of the dye complex into a newly designed mesoporous silica was accomplished via sol-gel process, where by the dye settled within silica pores as a guest. The photoluminescence properties of the dye-silica hybrid have been investigated in comparison with free dye in different solutions. A significant effect of the silica network has been observed on the excitations, emission, lifetimes and fluorescence quantum yields of the encapsulated dye molecules. The -O-Si-O- chain present in the silica was found to be responsible for increasing the mechanical and thermal strength of the encapsulated dye molecules and consequently preventing the dye against the effect of aggregation and quenchers

ACKNOWLEDGMENT

This work was supported by Tertiary Education Trust Fund (TETFUND) through Isa kaita college of Education Dutsinma, Katsina State Nigeria. We also acknowledged the contributions of Dr. Fabio Cucinotta from the Department of Chemistry, University of Newcastle.

REFERENCES

- Antina, E. V., Bumagina, N. A., V'Yugin, A. I., & Solomonov, A. V. (2017). Fluorescent indicators of metal ions based on dipyrromethene platform. *Dyes and Pigments*, *136*, 368-381. <https://doi.org/https://doi.org/10.1016/j.dyepig.2016.08.070>
- Badamasi, S., Tanko, Y. A., Yamusa, Y. A., Garba, N. N. & Najamuddeen Musa, M. (2020). Thermally stable dysprosium doped zinc-sodium-tellurite glasses: absorption and emission properties enhancement. *FUDMA Journal of Sciences (FJS)* ISSN online: 2616-1370 ISSN print: 2645 - 2944 Vol. 4 No. 1, March, 2020, 190 –1999
- Béziau, A., Baudron, S. A., Guenet, A., & Hosseini, M. W. (2013). Luminescent Coordination Polymers Based on Self-Assembled Cadmium Dipyrin Complexes. *Chemistry–A European Journal*, *19*(9), 3215-3223.
- Binnemans, K. (2009). Lanthanide-Based Luminescent Hybrid Materials. *Chemical Reviews*, *109*(9), 4283-4374. <https://doi.org/10.1021/cr8003983>

- Bodio, E., & Goze, C. (2019). Investigation of B-F substitution on BODIPY and aza-BODIPY dyes: Development of B-O and B-C BODIPYs. *Dyes and Pigments*, *160*, 700-710. <https://doi.org/https://doi.org/10.1016/j.dyepig.2018.08.062>
- Davila, J., Harriman, A., & Milgrom, L. R. (1987). A light-harvesting array of synthetic porphyrins. *Chemical Physics Letters*, *136*(5), 427-430. [https://doi.org/https://doi.org/10.1016/0009-2614\(87\)80280-4](https://doi.org/https://doi.org/10.1016/0009-2614(87)80280-4)
- Devaux, A., Calzaferri, G., Belser, P., Cao, P., Brühwiler, D., & Kunzmann, A. (2014). Efficient and Robust Host–Guest Antenna Composite for Light Harvesting. *Chemistry of Materials*, *26*(23), 6878-6885. <https://doi.org/10.1021/cm503761q>
- Dudina, N. A., Antina, E. V., Guseva, G. B., & Vyugin, A. I. (2014). The High Sensitive and Selective “Off-On” Fluorescent Zn²⁺ Sensor Based on the Bis(2,4,7,8,9-pentamethyldipyrrolylmethene-3-yl)methane. *Journal of Fluorescence*, *24*(1), 13-17. <https://doi.org/10.1007/s10895-013-1278-7>
- Fang, Y., Ma, Y., Zheng, M., Yang, P., Asiri, A. M., & Wang, X. (2018). Metal–organic frameworks for solar energy conversion by photoredox catalysis. *Coordination Chemistry Reviews*, *373*, 83-115. <https://doi.org/https://doi.org/10.1016/j.ccr.2017.09.013>
- Farràs, P., & Cucinotta, F. (2017). Recent advances in artificial photosynthetic systems at Newcastle University. *Comptes Rendus Chimie*, *20*(3), 272-282. <https://doi.org/https://doi.org/10.1016/j.crci.2015.11.025>
- Insuwan, W., Jungsuttivong, S., & Rangriwatananon, K. (2015). Host–guest composite materials of dyes loaded zeolite LTL for antenna applications. *Journal of Luminescence*, *161*, 31-36. <https://doi.org/https://doi.org/10.1016/j.jlumin.2014.12.031>
- Jarman, B. P., & Cucinotta, F. (2015). Photoactive amphiphiles for the assembly of supramolecular architectures [10.1039/C5FD00081E]. *Faraday Discussions*, *185*(0), 471-479. <https://doi.org/10.1039/C5FD00081E>
- Król, M. (2019). Hydrothermal synthesis of zeolite aggregate with potential use as a sorbent of heavy metal cations. *Journal*

- of *Molecular Structure*, *1183*, 353-359. <https://doi.org/https://doi.org/10.1016/j.molstruc.2019.02.011>
- Kumar, S., Malik, M. M., & Purohit, R. (2017). Synthesis Methods of Mesoporous Silica Materials. *Materials Today: Proceedings*, *4*(2, Part A), 350-357. <https://doi.org/https://doi.org/10.1016/j.matpr.2017.01.032>
- Leśniewski, A. (2016). Hybrid organic–inorganic silica based particles for latent fingerprints development: A review. *Synthetic Metals*, *222*, 124-131. <https://doi.org/https://doi.org/10.1016/j.synthmet.2016.03.032>
- Li, H., Fu, Y., Zhang, L., Liu, X., Qu, Y., Xu, S., & Lü, C. (2012). In situ route to novel fluorescent mesoporous silica nanoparticles with 8-hydroxyquinolate zinc complexes and their biomedical applications. *Microporous and Mesoporous Materials*, *151*, 293-302. <https://doi.org/https://doi.org/10.1016/j.micromeso.2011.10.021>
- Matsuoka, R., & Nabeshima, T. (2018). Functional Supramolecular Architectures of Dipyrrin Complexes. *Frontiers in chemistry*, *6*, 349-349. <https://doi.org/10.3389/fchem.2018.00349>
- Ramanjaneya Reddy, G., & Balasubramanian, S. (2015). Synthesis, characterization and photocatalytic studies of mesoporous silica grafted Ni(ii) and Cu(ii) complexes [10.1039/C5RA07469J]. *RSC Advances*, *5*(66), 53979-53987. <https://doi.org/10.1039/C5RA07469J>
- Rohand, T., Dolusic, E., Ngo, T. H., Maes, W., & Dehaen, W. (2007). Efficient synthesis of aryldipyrrmethanes in water and their application in the synthesis of corroles and dipyrromethenes. *Arkivoc*, *10*, 307-324.
- Sazanovich, I. V., Kirmaier, C., Hindin, E., Yu, L., Bocian, D. F., Lindsey, J. S., & Holten, D. (2004). Structural Control of the Excited-State Dynamics of Bis(dipyrrinato)zinc Complexes: Self-Assembling Chromophores for Light-Harvesting Architectures. *Journal of the American Chemical Society*, *126*(9), 2664-2665. <https://doi.org/10.1021/ja038763k>
- Shoji, S., & Tamiaki, H. (2019). Supramolecular light-harvesting antenna system by co-aggregates of zinc (bacterio)chlorophyll-a derivatives with biomimetic chlorosomal self-assemblies. *Dyes and Pigments*, *160*, 514-518. <https://doi.org/https://doi.org/10.1016/j.dyepig.2018.08.026>
- Tolbin, A. Y., Pushkarev, V. E., Tomilova, L. G., & Zefirov, N. S. (2017). Threshold concentration in the nonlinear absorbance law [10.1039/C7CP01514C]. *Physical Chemistry Chemical Physics*, *19*(20), 12953-12958. <https://doi.org/10.1039/C7CP01514C>
- Vecchi, A., Galloni, P., Floris, B., Dudkin, S. V., & Nemykin, V. N. (2015). Metallocenes meet porphyrinoids: Consequences of a “fusion”. *Coordination Chemistry Reviews*, *291*, 95-171. <https://doi.org/https://doi.org/10.1016/j.ccr.2015.02.005>
- Yu, Y., Zhang, Y., Jin, L., Chen, Z., Li, Y., Li, Q., Cao, M., Che, Y., Dai, H., Yang, J., & Yao, J. (2019). Photoelectricity and thermoelectricity in organic chlorophyll phototransistors. *Organic Electronics*, *65*, 381-385. <https://doi.org/https://doi.org/10.1016/j.orgel.2018.11.039>



©2023 This is an Open Access article distributed under the terms of the Creative Commons Attribution 4.0 International license viewed via <https://creativecommons.org/licenses/by/4.0/> which permits unrestricted use, distribution, and reproduction in any medium, provided the original work is cited appropriately.